16th World Conference on Earthquake, 16WCEE 2017
Santiago Chile, January 9th to 13th 2017
Paper N° 1373 (Abstract ID)
Registration Code: S-U1464737382

# TESTING AND MODELLING OF PROTOTYPE TENSION-ONLY SEISMIC ENERGY DISSIPATION DEVICES

J. Cook[1], G.W. Rodgers[2], G.A. MacRae[3] & J.G. Chase[4]

[1] PhD Candidate, University of Canterbury, Christchurch, New Zealand, jarrod.cook@pg.canterbury.ac.nz
[2] Senior Lecturer, University of Canterbury, Christchurch, New Zealand, geoff.rodgers@canterbury.ac.nz
[3] Associate Professor, University of Canterbury, Christchurch, New Zealand, gregory.macrae@canterbury.ac.nz
[4] Distinguished Professor, University of Canterbury, Christchurch, New Zealand, geoff.chase@cantebury.ac.nz

## Abstract

Seismic damage-resistant structures, such as jointed precast connections and rocking wall structures, usually require supplementary energy dissipation devices to limit structural and non-structural demands. A ratcheting, tension-only device has been developed to offer resistance to loading in tension, while offering negligible resistance to compression, and can be used in conjunction with a range of energy dissipation mechanisms. This lack of compressive forces allows unimpeded re-seating of a rocking connection to minimise residual structural displacements. Upon re-loading, dissipater engagement will be more rapid due to the ratcheting mechanism, as the absence of residual compressive loads reduces the amount of elastic take-up before yielding occurs on subsequent cycles. A tension-only solution also removes the requirement for buckling restraint in the dissipater design. The design of the ratcheting mechanism was refined to provide ease of manufacture, eliminating complex and expensive processes, to reduce the overall construction costs.

Experimental proof-of-concept testing on 14 yielding-steel dissipaters, providing a yield force of 45kN and an ultimate tensile force of 65kN, was used to demonstrate the function of two prototype ratcheting mechanisms and assess the hysteretic behaviour of the dissipater element and the overall system. Results show rapid and reliable engagement in both prototypes. The ratcheting mechanism can potentially induce large inelastic displacement demands within the dissipater, and simplified methods are required to define this demand. A spectral analysis has been completed to assess the effects of the device on the response of a SDOF structure model to a range of ground motion recordings. A linear relationship between spectral displacement and cumulative inelastic demand on the dissipater element is revealed for lower peak displacements. The highest ratio of cumulative inelastic dissipater demand to the peak displacement was 3.3, with the majority of results having ratios of less than 2.0.

*Keywords: Grip 'n' grab; tension-only; energy dissipation; prototype device; inelastic demand*

## 1. Introduction

The capital cost of the Canterbury earthquakes of 2010 and 2011 has been estimated to be as high as $40 billion [1]. The extent of the damage and operational disruption has led to an increased public expectation regarding the resilience of structures to earthquakes. Low damage structural technology is a large field covering much of the work towards improving building performance levels following seismic events [2].

A key concept in this technology is the idea of providing specific energy dissipation mechanisms to absorb earthquake energy and reduce the damage to a structure. Metallic dampers or yielding steel dissipaters remain a desirable option due to the familiarity of the behaviour of steel under loading, and their general simplicity in design. However, a key issue with some common approaches, such as with buckling restrained braces (BRBs), is the presence of residual compressive stresses after a seismic event. Such stresses limit the effectiveness of the device to allow the centring of a structure post-earthquake, and also impair their performance in subsequent loading cycles.

Slender bracing that yields in tension and buckles elastically in compression partially removes these residual compressive forces. However, plastic deformation on prior cycles increases the unstressed member length and results in a dead-zone with take-up on subsequent cycles. Therefore, subsequent cycles will provide delayed engagement and reduced energy dissipation capacity.

One way to address these issues is the use of a tension only mechanism, where dissipation occurs due to mechanisms such as yielding or friction. This concept, originally referred to as a Grip ‘n’ Grab (GnG) device, was modelled for a rocking system [3]. However, it was only a computational investigation and no physical prototype or design details were investigated. This paper outlines the design, testing and modelling that has been completed with two prototype devices.

Other tension-only damper and bracing research considered hysteretic dampers [4] and seesaw systems [5]. Recent research produced newer developments, including adding self-centring capability to BRB systems [6], using wedge spring devices to offset anchor bolt elongation in column connections [7] and a non-buckling segmented brace system with sliding joints [8]. However, the proposed device and prototype presented in this work offers a novel alternative that aims to be a simple, cost-effective solution for industry.

## 2. Device Design

Two prototype GnG ratcheting devices were designed, manufactured and tested, with the two designs showing a progression of functionality and use of space. The first GnG device makes use of a linear ratcheting mechanism to achieve the desired single direction engagement. This mechanism allows the device to engage in tension, offering resistance to motion acting to displace a structure, while providing negligible impediment to any restoring motion. A number of concepts were considered for the ratchet mechanism including designs making use of friction-based or stepped interfaces. Particular attention was given to reliable engagement, low manufacturing cost and robustness of the design concepts.

Fig. 1a shows the assembly of the first prototype. The initial chosen design is comprised of two pawls and a rack with teeth on both sides. A tension spring fitted between the pawls is used to aid initial engagement during tensile loading. Upon initial engagement the ratchet mechanism locks tighter as the engagement interface is self-stabilising and the tension spring provides initial engagement only. The two pawls rotate about pins located within a main support body made from a standard RHS section.

A circular yielding steel dissipater was attached to the rack component to provide energy dissipation in the initial testing. Each end of the device has a rectangular tongue for mounting in the MTS-810 test machine. Tensile forces in the dissipater are transferred to the rack, which induces compressive forces in the pawls. These forces then transfer into the main support body via bearing contact areas on the pawl pins. Cap screws connect the cover plate with the main support body and the upper tongue. These components are shown in Fig. 1a.

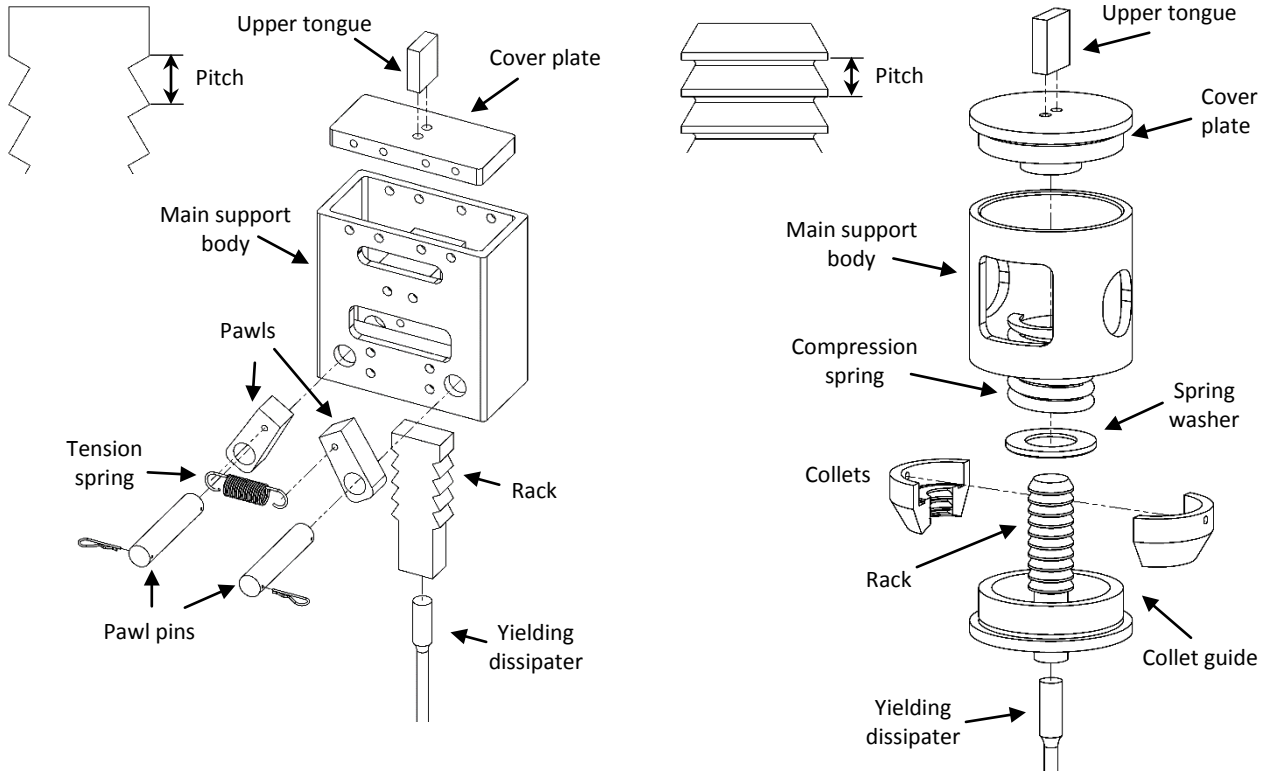


Fig. 1 – a) First, linear ratchet mechanism assembly; and b) Second, axisymmetric prototype. Pitch dimensions are shown in inserts.

The second generation prototype, in Fig. 1b, features an axisymmetric design. This arrangement supports a greater contact area, enabling a reduced tooth pitch and more rapid engagement, with less take-up on initial loading or re-loading. A compression spring acts upon two collets which tighten around a circular rack. The action of these collets replaces the role of the pawls used in the first design. Tensile forces in the dissipater are transferred through the rack into compressive forces in the collets, and then into the tapered collet guide. Threaded connections are used to connect the collet guide and cover plate to the main support body. The mounting arrangements used with the prototype designs are specific to the hydraulic testing apparatus, and do not limit the possible connection types and applications for the device in service.

Racks of four different pitch sizes have been used during the testing of the two prototypes. Pitches of 40 mm and 20 mm were used with the first prototype to establish the concept, while reduced pitches of 10 mm and 3 mm were used with the more advanced, second device. Both prototypes utilise a self-stabilising engagement mechanism, where a spring force is used to provide initial engagement before tensile loading forces provide an increased clamping force, ensuring robust and reliable engagement in field structures.

## 3. Experiments and results

### 3.1 Test apparatus and data acquisition

Experimental proof-of-concept testing on a total of fourteen dissipater elements was used to demonstrate the function of the ratcheting mechanism and assess the hysteretic behaviour of the dissipater element and the overall device, for both prototypes. High speed camera footage of the ratcheting mechanism was recorded to assess engagement timing with two different pitch sizes for the first, linear prototype. A series of monotonic and cyclic tests were completed with both prototypes in an MTS-810 test machine using the setup shown in Fig. 2.

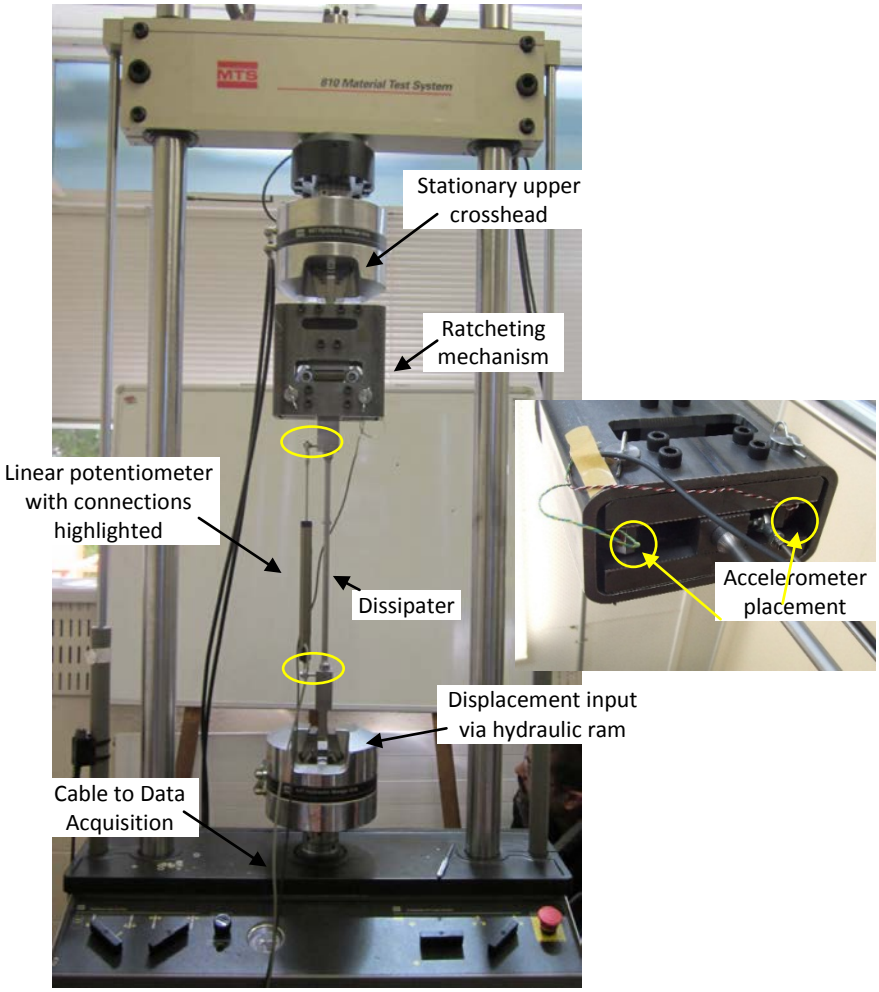


Fig. 2 – Initial GnG prototype test apparatus, with accelerometer placement shown in insert.

A data acquisition system recorded five outputs against time during the experiments. The force and displacement of the hydraulic ram, at the lower end of the device, were recorded from the test machine. Note that the upper crosshead remained stationary. A linear potentiometer position sensor was used to record changes in the length of the dissipater element, and was mounted to the device via rod ends bolted to the lower region of the rack and the upper end of the lower tongue, as shown in Fig. 2. The remaining two signals were taken from a pair of single-axis accelerometers mounted on the lower ends of the two pawls, shown in the insert in Fig. 2.

These accelerometers were used to capture acceleration spikes during ratcheting, which could be used to assess pawl engagement timing. Ratcheting produces small acceleration spikes upon impact between the rack and pawls. All data was sampled at 1000 Hz to ensure all frequencies were captured. High speed camera footage was recorded for several of the tests with the first prototype to measure pawl engagement time using a FASTCAM SA5 model 775K-C3 camera operating at 1000 fps.

### 3.2 Cyclic testing

Cyclic tests were completed to assess the hysteretic behaviour of the dissipater element and the overall device. A summary of the cyclic testing parameters is presented in Table 1. The results are shown in Table 2, including the maximum compressive forces recorded. Test amplitudes were selected to clearly present a single ratcheting action during each compressive loading cycle, with the exception of the 3 mm pitch test using an amplitude of 10 mm. This amplitude was chosen to provide a comparison with the behaviour from the 10 mm tooth pitch experiments with the same input displacement amplitude. This comparison is presented in Section 4. Values from repeated experiments with the same test parameters are separated by a comma.

Table 1 – Summary of cyclic testing parameters

| Ref. | Prototype No. | Pitch (mm) | Amplitude (mm) | Frequency (Hz) | No. Cycles |
|---|---|---|---|---|---|
| C40-025 | 1 | 40 | 25 | 0.25 | 2 |
| C40-050 | | | | 0.50 | 2 |
| C20-025 | | 20 | 15 | 0.25 | 3, 3, 3 |
| C20-050 | | | | 0.50 | 3 |
| C10-050 | 2 | 10 | 10 | 0.50 | 5, 6 |
| C10-100 | | | | 1.00 | 5, 6 |
| C10-150 | | | | 1.50 | 5, 5 |
| C03-050 | | 3 | 10 | 0.50 | 4 |
| C03-051 | | | 5 | 0.50 | 17 |

Table 2 – Summary of cyclic testing results

| Ref. | Yield Force (kN) | Ultimate Tensile Force (kN) | Dissipater Elongation to Fracture (mm) | Max. Compressive Force (kN) |
|---|---|---|---|---|
| C40-025 | 44.1 | 66.7 | 75.2 | 1.27 |
| C40-050 | 46.0 | 67.1 | 71.4 | 0.53 |
| C20-025 | 42.4, 43.5, 46.5 | 65.1, 65.3, 65.0 | 65.2, (59.2)*, (59.3) | 0.30, 0.35, 0.28 |
| C20-050 | 49.9 | 65.7 | 71.4 | 0.49 |
| C10-050 | 43.3, 43.2 | 65.9, 66.2 | (48.3), 63.1 | 0.75, 0.84 |
| C10-100 | 42.9, 43.8 | 66.0, 66.6 | (48.9), 62.7 | 0.81, 0.73 |
| C10-150 | 43.3, 45.0 | 66.5, 66.2 | (48.5), 56.9 | 0.74, 0.80 |
| C03-050 | 41.5 | 66.2 | 57.5 | 0.46 |
| C03-051 | 40.7 | 64.3 | 60.9 | 0.32 |

*In Table 2, parentheses indicate elongation of dissipaters that did not fracture during testing. These tests consisted of fewer cycles, and insufficient plastic displacement occurred to fracture the yielding steel dissipater element, resulting in significantly lower values in some cases.

The maximum compressive force experienced by the device during any of the cyclic loading experiments was 1.27 kN. This result occurred during a test with the first, linear prototype using a 40 mm pitch rack and operating at 0.25 Hz. The largest compressive force produced by the second, axisymmetric prototype from the cyclic testing was 0.84 kN. In all tests the compressive forces are very low, as intended by design. In particular, in these specific tests the maximum compressive forces are ~1-2% of the ultimate tensile forces.

The experimental values show a reasonable consistency, with an average yield force of 44.0 kN and an average ultimate tensile force of 65.9 kN. Any differences are thus likely due to natural manufacturing or test variation. The average elongation to fracture was 64.9 mm. This result represents ~ 72% of the expected 90 mm elongation at break, indicating that the assumed uniform plastic strain throughout the entire dissipater length may

not have been obtained during testing. Hence, fracture loads were lower than theoretically calculated, a factor to consider in any dissipater design or application.

Hydraulic test machine limitations, most notably a maximum force of 100 kN, dictated the maximum dissipater diameter for testing. The ratcheting mechanism is capable of much larger forces if required and exhibited no visible signs of yielding or other damage following testing. While these results use yielding steel dissipaters, various dissipation methods, such as friction connections [9] and lead dissipaters [10], could be implemented with the ratcheting mechanism as required for specific applications and force or yield levels. Most importantly, these specific tests were only designed to validate the functionality of the GnG device, which was demonstrated, and is not specific to the yielding steel dissipater.

## 4 Hysteretic device behaviour

The effect of the ratcheting mechanism produces a unique hysteresis loop for the behaviour of the system. A force displacement plot of the testing with the first prototype, during the cyclic tests with the 20 mm pitch rack, is presented in Fig. 3. The input displacement amplitude is 15 mm. The hysteresis loops begin in typical fashion, displaying elastic behaviour, yielding and strain hardening before the first load reversal. During the compressive loading there is an elastic recovery region followed by a period of negligible force. The bottom of the hysteresis loop lies essentially on the horizontal axis, indicating that only very small compressive force is induced during the unloading phase of the cycle.

The 30 mm peak-to-peak displacement, equal to twice the amplitude of the cyclic loading input (2A), exceeds the combined value of the tooth pitch of the rack (p) and the elastic displacement of the dissipater ($\delta_{elastic}$). As a result, the displacement at which the GnG device engages during the next loading cycle is offset by an amount equal to the tooth pitch. This effect is shown in Fig. 3. During the unloading phase of the initial cycle, zero force is achieved at a displacement of approximately 13 mm, indicating approximately 2 mm of elastic recovery from the 15 mm displacement peak. Subsequent to ratcheting, during the following cycle the onset of elastic strain behaviour of the system occurs at a displacement of approximately - 7 mm, with respect to the initial position.

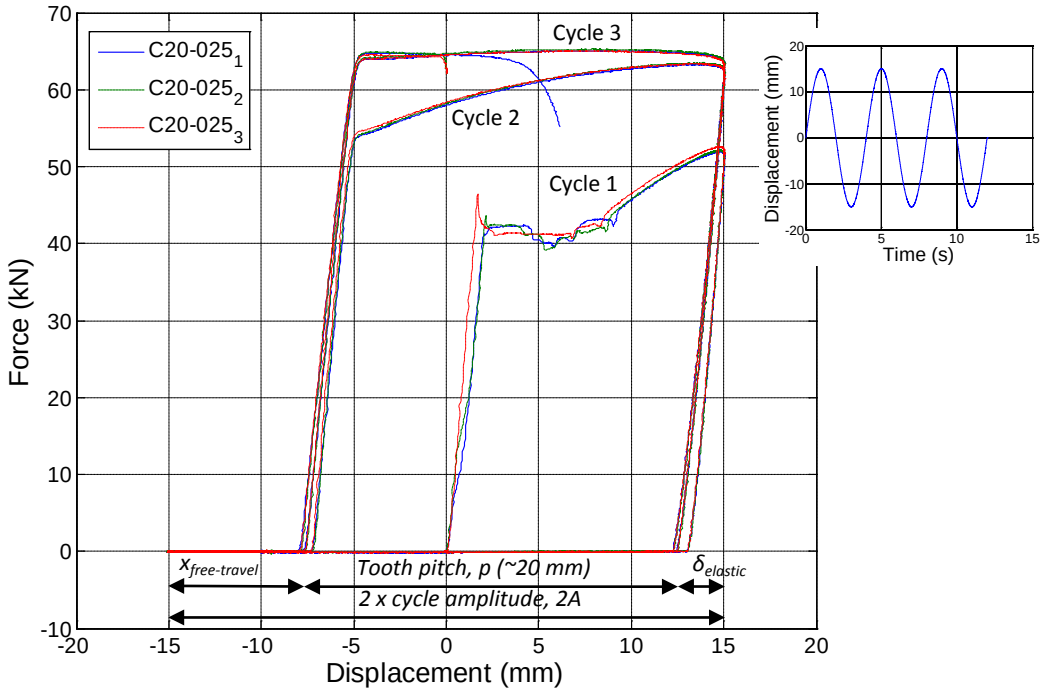


Fig. 3 – Force-displacement hysteresis loops for cyclic testing of 20 mm pitch rack, with input displacement profile inset

Similar behaviour occurs for the other two loading and unloading cycles, with a slight offset in position. This slight shifting of the response is due to an increase in elastic displacement within the device as a result of the increased force within the yielding steel element from strain hardening. The hydraulic ram reaches a minimum position of -15 mm, and Fig. 3 indicates that up to 8 mm of free-travel ($x_{free\text{-}travel}$) exists before engagement of the rack and pawls resumes after the load reversal. Similar behaviour was exhibited in tests with the larger 40 mm pitch rack, with around 7 mm of free-travel upon reloading.

In Fig. 3 from a displacement of -15 mm to -7.5 mm, reloading occurs with negligible resistive force. This free-travel is directly proportional to tooth pitch and can be approximated by Eq. (1), where it is assumed that $p < (2A - \delta_{elastic}) < 2p$:

$$x_{free\text{-}travel} = 2A - \delta_{elastic} - p \quad (1)$$

where A is the amplitude of the displacement input cycle and $\delta_{elastic}$ is the elastic recovery displacement of the device during unloading, and p is the tooth pitch. These terms are expressed on Fig. 3. Multiple ratcheting actions can occur when $(2A - \delta_{elastic}) > 2p$. The engagement displacement values are consistent for tests with the same rack due to approximately equal starting positions. In particular, the rack rests on the closed pawls at the start of the test.

The results presented in Fig. 3 differ from the expected behaviour of a regular yielding steel hysteresis loop due to the ratcheting mechanism essentially shifting the zero displacement datum. The amount of free-travel prior to re-engagement of the yielding mechanism on subsequent cycles is reduced due to the absence of compressive loads. The input displacement does not need to exceed that experienced on prior cycles before energy dissipation can occur, which is a limitation with simple tension bracing that is ameliorated here by the GnG device. While the test was cyclic, the steel yields only in tension and the behaviour of the steel dissipater approximates a piecewise version of a standard monotonic tensile test.

Fig. 4 compares the hysteretic behaviour of the second prototype using two different pitch sizes, 10 mm and 3 mm, for cyclic loading with an input displacement amplitude of 10 mm. This data is from tests C10-050, with 10 mm pitch, and C03-050, with 3 mm pitch, respectively. Both tests were completed at a frequency of 0.5 Hz.

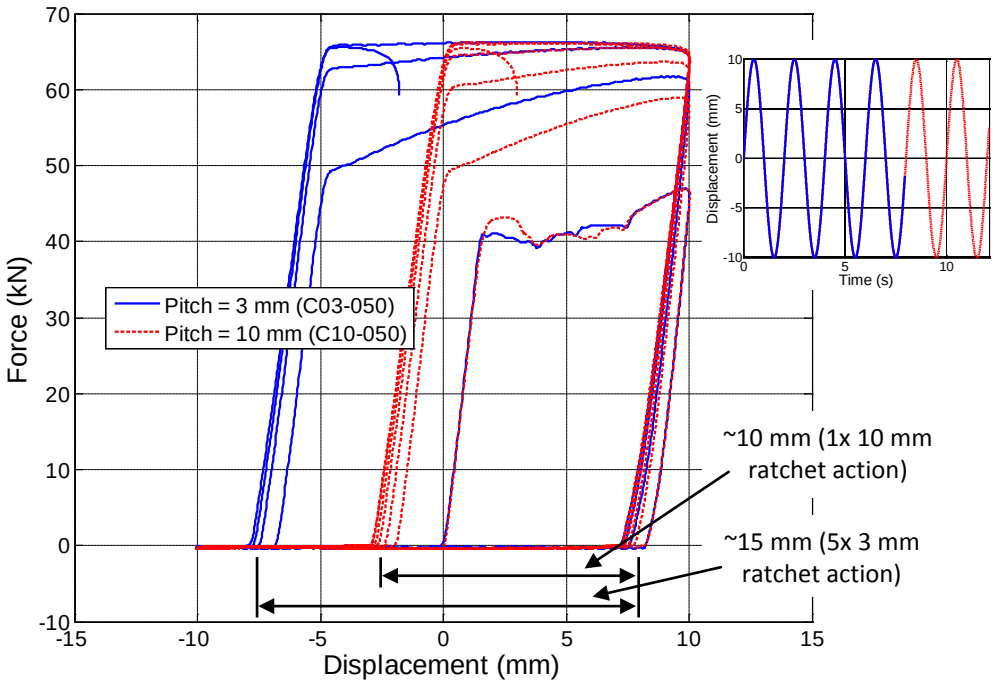


Fig. 4 – Comparison of free-travel reduction and increased energy dissipation with use of finer pitch rack in

second prototype. Displacement inputs are shown inset.

On subsequent loading cycles the re-engagement of the device with the 10 mm pitch rack and collets occurs at a displacement of approximately -3 mm, with respect to the initial position. This engagement displacement is changed to approximately -7 mm when using the finer 3 mm pitch rack, representing a reduction from 7mm to 3mm in the free-travel that occurs prior to engaging the energy dissipation mechanism, as expected with the finer pitch rack. The offset in engagement position with the 10 mm pitch setup is ~10 mm, representing a single ratchet action for each compressive loading cycle. This shift in engagement is increased to around 15 mm when using the 3 mm pitch rack and collets, which accounts for five ratchet actions in each cycle. The enclosed area for the finer pitched rack has thus increased by ~50%, demonstrating a significant increase in energy dissipation for the same displacement loading input. Additional cycles were required to achieve fracture with the larger pitch, as shown in the input displacements inset in Fig. 4, due to the greater free-travel and reduced inelastic action, and hence reduced energy dissipation, in each cycle with the larger pitch rack. Overall, as expected, the finer pitch led to less free-travel and thus greater energy dissipation.

## 5. Spectral analysis

### 5.1 Simulation details

A computational hysteresis model was created to replicate the experimental GnG behaviour using MATLAB® software (The MathWorks Inc. 2014). This model was then added to a single degree of freedom (SDOF) structure model to simulate the effect of the GnG device on structural response to earthquake loading. The implemented model simulates the use of two GnG devices to limit the structural response. In the model, one GnG device is attached to either side of the structure and each device provides resistive forces for displacements of the structure in either the positive or negative direction, relative to the initial resting point.

This setup is used as a simplified analogy for a rocking wall system, where a GnG device could be mounted to each side of the rocking wall. The device located on the side nearest to the rocking edge will not experience any change in length, while the device on the side opposite to the rocking edge will be engaged. Only one of the two devices is active at any time, avoiding interference between them. This simple model is used to provide a first approximation of important relationships in the response of the structure and the behaviour and capacity of the GnG device.

A spectral analysis was completed to assess the impact of GnG devices with different yield force and stiffness parameters on the behaviour of a model structure exposed to a range of earthquake ground motion recordings. Three suites of 20 earthquake recordings from the SAC project [11] were used to create a response spectra for the structure model. The low, medium, and high suites represent ground motions having probabilities of exceedance of 50% in 50 years, 10% in 50 years, and 2% in 50 years, respectively.

The simulations were run for a range of structures with different natural periods, ranging from 0.1s to 5.0s, and for a variety of GnG systems with different dissipater yield force and stiffness variations. The yield force was varied as a portion of the seismic weight of the model structure. Values of 10%, 20%, 30%, 40% and 50% of the seismic weight, W, were used for the yield force, $F_{yield}$. The pre-yield stiffness of the dissipater in the GnG devices, $K1_{GnG}$, was varied in relation to the model structure stiffness, k. Values of 1, 2, 5 and 10 times k were used for the initial elastic dissipater stiffness.

Rayleigh damping of 5% was modelled in the linear structure and the mass was kept constant. Variation in the structure stiffness was used to achieve the required range of structure periods. A constant tooth pitch of 20 mm was used across all simulations. This study was used to recognise the sensitivity of the system response to changes in important design parameters and to determine how the most favourable behaviour could be obtained.

### 5.2 Structural response

Fig. 5 shows a sample of the spectral analysis results obtained for the SAC medium earthquake ground motion suite. Geometric mean displacement response spectra and associated multiplicative factors of the response, when compared to the nominal structure response, are presented. In the response spectra plots on the left, the natural

period of the model structure is plotted against the geometric mean of the spectral displacement from all of the 20 earthquake recordings in the medium suite. The response of the model structure without any GnG devices, or any other augmentation, is indicated as the nominal response in these plots.

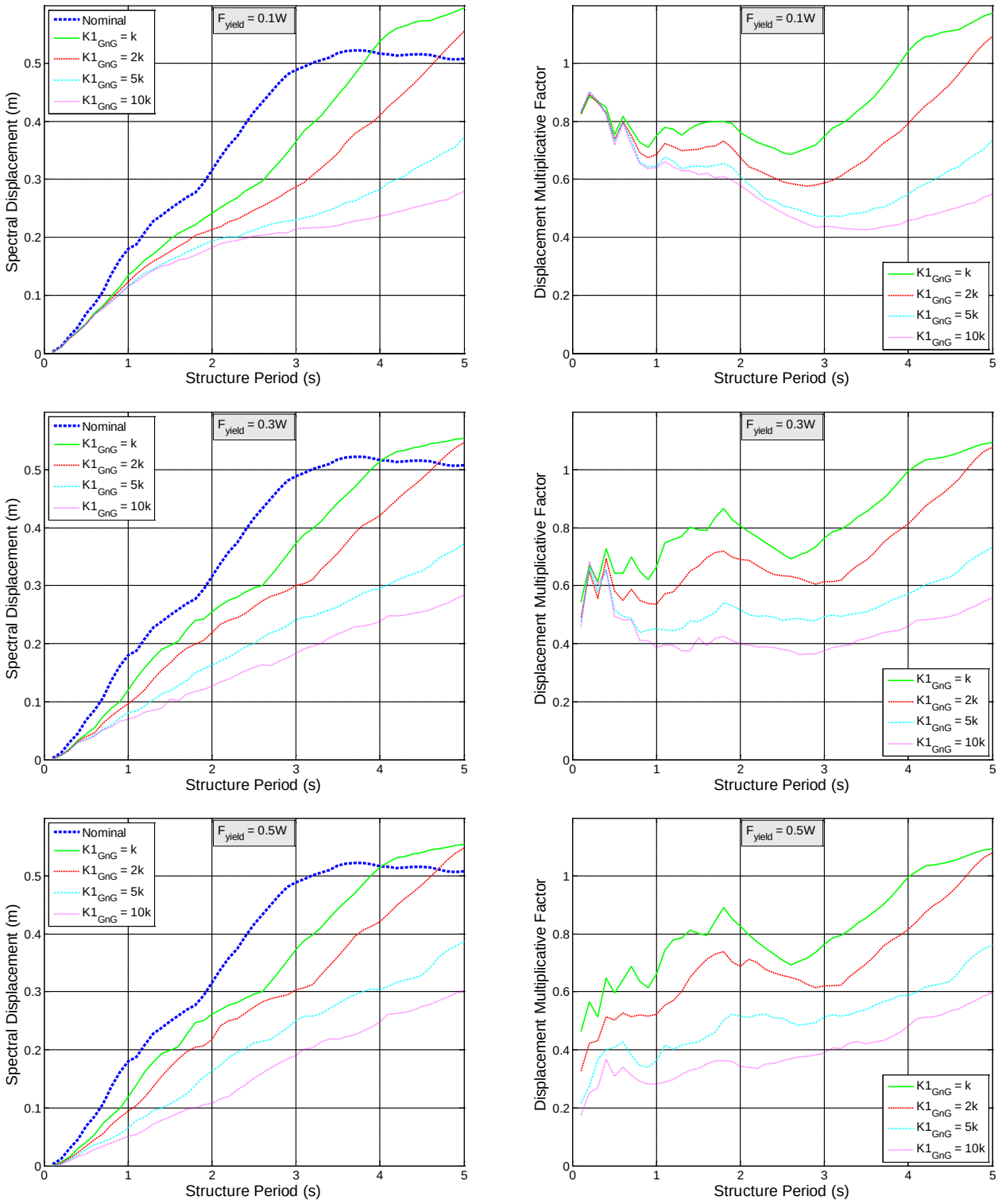


Fig. 5 – Geometric mean displacement response spectra and associated multiplicative factors for medium suite earthquake recordings with several variations of dissipater pre-yield stiffness and yield force

Multiplicative factors were calculated for the geometric mean response spectra and are shown in the plots on the right of Fig. 5. The multiplicative factors presented here are found by dividing the geometric mean of the augmented structure response by the geometric mean of the nominal structure response, for the indicated variations of device dissipater parameters. Many variations of these parameters are simulated to explore the combinations that provide the best structural response. The grey annotation box and the legend indicate the values of the dissipater yield force and pre-yield stiffness, respectively, with respect to the variables of the model structure as discussed in Section 5.1.

Reductions in peak displacements in augmented structures are shown in Fig. 5 where the multiplicative factors are less than unity. High dissipater stiffness produces the most significant reductions in peak displacement. The use of GnG devices with 10 times the structure stiffness achieved multiplicative factors of below 0.2 in some simulations with very short period structures. These multiplicative factors were higher for more practical structure periods. For a structure period of 1.0 seconds, the peak displacement was reduced to as little as 30% of the nominal value. This result is for a dissipater yield force of half the seismic weight of the model structure, where greater elastic displacement occurs in the dissipater. This yield force value of 50% of the weight might be larger than is generally practical for many structures. However, the span of results from 10% to 50% is intended to cover the full range of likely designs. In general, smaller multiplicative factors were recorded for the GnG systems with larger yield forces.

### 5.3 Cumulative dissipater demand

The capacity of the dissipater required to operate for the duration of an earthquake, and to avoid early fracture of the dissipater in practice, can be obtained from the results of the individual time history analyses. A geometric mean of the cumulative inelastic dissipater displacement over the full length of each earthquake recording in the medium suite is presented in Fig. 6. These values are plotted against the peak spectral displacement recorded in the structure response.

In Fig. 6 some data points lie on the x axis. These results are from structures with longer periods, which recorded no inelastic dissipater displacement. This absence of inelastic action is due to the reduced structure stiffness required to achieve the longer structure periods when using a fixed mass approach, as described in Section 5.1. The low stiffnesses allow for greater displacement prior to the onset of inelastic behaviour in the dissipater, reducing the inelastic displacement demand. Less inelastic dissipater displacement is recorded for larger yield forces in the dissipater. This meets expectations due to the associated delay in the onset of yielding of the dissipater. There is an increased elastic take-up due to the higher dissipater yield force and larger displacements are required to achieve inelastic behaviour.

For spectral displacements of less than ~0.1 m, there is an approximately linear relationship between the spectral displacement and the cumulative inelastic displacement demand in the dissipater. In most cases where the dissipater was yielded, the cumulative demand was less than twice the spectral displacement. However, the maximum ratio between the cumulative inelastic demand and the peak displacement was 3.3. This result is from the lowest dissipater yield force applied in the study, which was 10% of the seismic weight of the structure model.

Dissipaters modelled with greater stiffness produced greater total inelastic dissipater displacement. This result matches reasonable expectation due to the more rapid onset of inelastic behaviour over shorter displacements. In general, increased energy dissipation, as a result of greater plastic deformation in the dissipater, is recorded for stiffer dissipaters designed with lower yield forces. A greater cumulative demand on the dissipater indicates a higher level of energy absorbed from the earthquake ground motion. This reduces the demand on the structure. In practice dissipaters will need to be carefully designed to handle the extra loading and remain active for the duration of the earthquake to protect the structure.

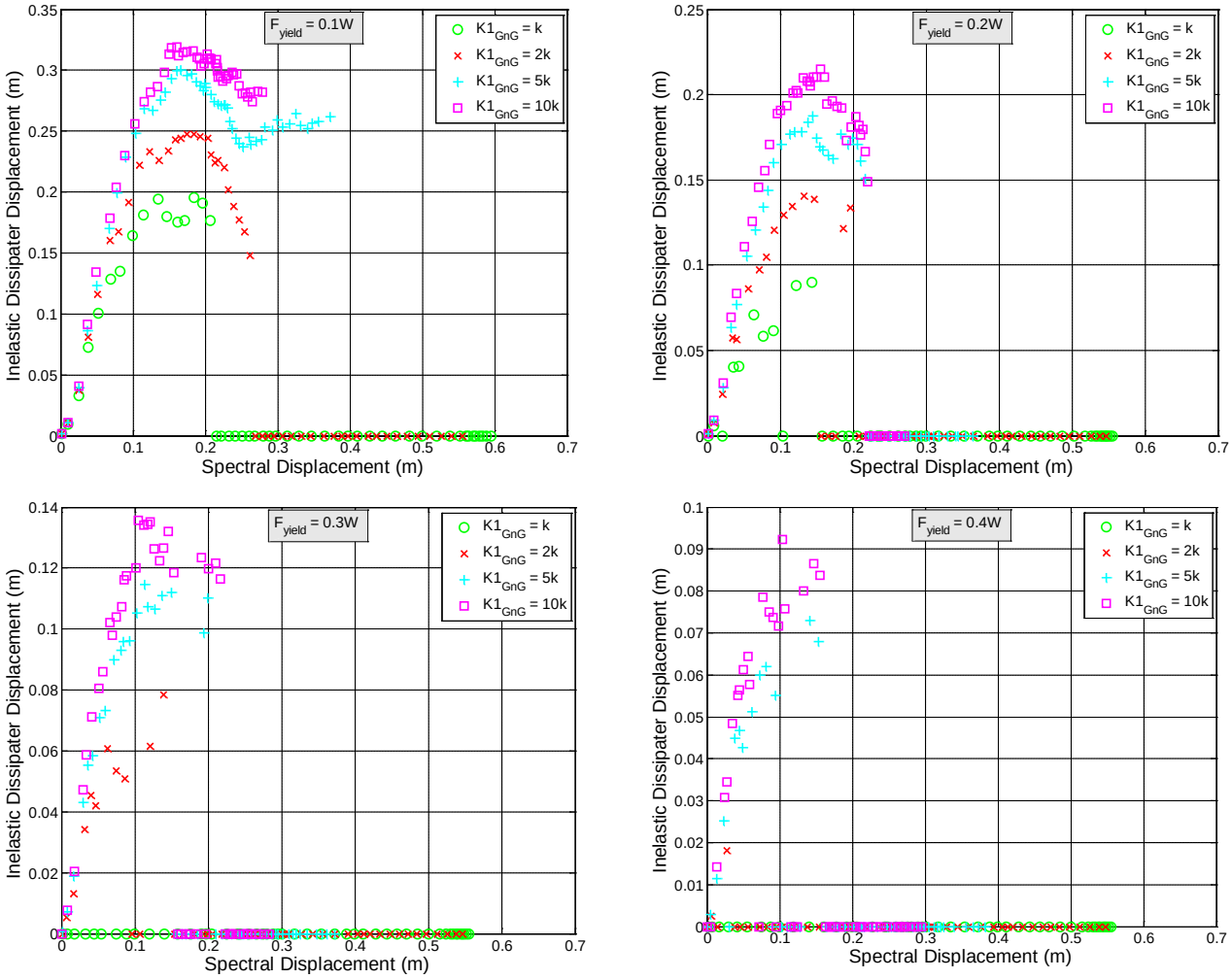


Fig. 6 – Geometric mean inelastic dissipater displacement response spectra for medium suite earthquake recordings with several variations of dissipater stiffness and yield force

## 6. Conclusions

A ratcheting, tension-only dissipater device has been developed to offer resistance to loading in tension, while offering negligible resistance to compressive motion. This lack of compressive forces allows re-seating of a rocking connection and minimises residual structural displacements. Upon reloading, dissipater engagement will be more rapid than a simple steel dissipater due to the ratcheting mechanism, as the absence of residual compressive loads reduces the amount of elastic take-up before yielding occurs. This faster response will reduce impact loads and maximise the amount of energy absorbed by the device, thus minimising the response of the structure and the effects of earthquake loading.

A hysteresis model has been developed to capture the behaviour of the Grip 'n' Grab ratcheting dissipater mechanism and has been used to assess the effect on structural response and the cumulative inelastic displacement demand in the dissipater. Spectral analysis using a SDOF structural model to simulate the effect of a pair of GnG devices on the system response to a range of earthquake ground motions indicates that significant reductions in peak displacements of up to 70% can be achieved for a structure with a period of 1 second. In particular, this is achieved when using a dissipater with a stiffness of 10 times the structure stiffness. Yield force is shown to have a significant effect on reductions in peak displacements for structures with short periods below 1 second. There is greater cumulative displacement demand in the dissipater for stiffer dissipaters with lower

yield forces. The maximum ratio recorded between the cumulative inelastic demand and the peak displacement was 3.3.

This initial spectral analysis supplements the promising results from the cyclic testing of two prototype devices, and shows the potential for the Grip 'n' Grab system to reduce structural response and be a favourable option in supplemental damping and bracing systems. It will be important to carefully design dissipater capacity to meet specific structural demands. The results presented here are all for a single tooth pitch value, and the influence of tooth pitch on the structural response and dissipater demand is an important aspect of ongoing work. Implications on the absolute acceleration response should also be considered.

## 7. Acknowledgements

Financial support for the experimental work from the BRANZ Building Research Levy is gratefully acknowledged. Thanks also go to The Sir Robertson Stewart Scholarship, The Todd Foundation and the UC Quake Centre for their support. Furthermore, travel support from the New Zealand Earthquake Commission (EQC) and the Canterbury Branch, Royal Society of New Zealand (RSNZ) to present this paper is much appreciated.

## 8. References

[1] New Zealand Treasury. 2014. *2014 Budget: Budget Policy Statement.* Wellington, New Zealand.

[2] Canterbury Earthquakes Royal Commission. 2012. *Low-damage Building Technologies*. Christchurch, NZ.

[3] Gunning, M. & Weston, D. 2013. *Assessment of Design Methodologies for Rocking Systems*, ENCI493 Report, Supervised by MacRae, G.A., Dept of Civil and Natural Resources Eng, Univ of Canterbury, Christchurch, NZ.

[4] Phocas, M.C. & Pocanschi, A. 2003. Steel frames with bracing mechanism and hysteretic dampers. *Earthquake Engineering and Structural Dynamics*, 32(5): 811-825.

[5] Kang, J.D. & Tagawa, H. 2013. Seismic response of steel structures with seesaw systems using viscoelastic dampers. *Earthquake Engineering and Structural Dynamics*, 42(5): 779-794.

[6] Eatherton, M.R. Fahnestock, L.A. & Miller, D.J. 2014. Self-centering buckling restrained brace development and application for seismic response mitigation, *10th U.S. National Conference on Earthquake Engineering: Frontiers of Earthquake Engineering, NCEE 2014, Anchorage, Alaska, 21-25 July, 2014.*

[7] Lei, J.S. Luo, W.X. Jiang, J.L. Zhang, W. 2014. Seismic performance analysis of steel frame with wedge devices based on energy dissipation, *4th International Conference on Civil Engineering, Architecture and Building Materials, CEABM 2014, Haikou, China, 24-25 May, 2014.*

[8] Hao, H. 2015. Development of a New Nonbuckling Segmented Brace. *International Journal of Structural Stability and Dynamics*, 15(8): Article in Press.

[9] Clifton, G.C. 2005. *Semi-rigid joints for moment-resisting steel framed seismic-resisting systems*, PhD Thesis, The University of Auckland, Auckland, New Zealand.

[10] Rodgers, G.W. Solberg, K.M. Chase, J.G. Mander, J.B. Bradley, B.A. Dhakal, R.P. & Li, L. 2008. Performance of a damage-protected beam-column subassembly utilizing external HF2V energy dissipation devices, *Earthquake Engineering and Structural Dynamics*, 37(13): 1549-1564.

[11] Sommerville, P. Smith, N. Punyamurthula, S. & Sun, J. 1997. Development of ground motion time histories for phase II of the FEMA/SAC steel project. *SAC Background Document Report SAC/BD-97/04*